Dimensionality reduction and density-based clustering for transfer function design in Direct Volume Rendering

SIBGRAPI Paper ID: 99999

***Abstract*—Transfer functions (TFs) are a fundamental component of volume visualization and have been extensively studied in the context of Direct Volume Rendering (DVR). In the traditional DVR pipeline, TFs serve multiple roles, primarily material classification and mapping data values to optical properties. The effectiveness of a TF is closely tied to the characteristics of the underlying data. While multidimensional TFs offer increased classification capabilities, their design remains a complex task, especially when aiming to emphasize specific volume features. This paper presents an unsupervised volume classification method that facilitates both the definition and design of TFs. The proposed approach combines dimensionality reduction, clustering and pivot-based indexing to support the specification of meaningfulTFs. The results include a user-friendly volume exploration workflow based on initial TF parameters, a semi-automated classification mechanism, and an enhanced 2D scatterplot interface for interactive data analysis.**

I. Introduction

Direct Volume Rendering (DVR) is widely used in scientific and medical applications to visualize three-dimensional scalar data. A key element in DVR is the transfer function (TF), which maps volume data attributes (e.g., density) to visual properties such as color and opacity [1].

Multidimensional TFs can enhance data classification, but their design becomes increasingly complex with more input attributes [1], [2]. Since no universal TF fits all datasets, design is often manual and highly dependent on user expertise [3]. Dimensionality and non-intuitive parameter spaces further complicate the process.

We propose a low-cost, unsupervised approach to simplify TF design. Our method combines clustering, dimensionality reduction, and pivot-based indexing to support semi-automated classification. A modified 2D scatter plot interface facilitates intuitive exploration of volume features.

Our main contributions are:

- A computationally efficient method for generating TFs with minimal manual adjustment.
- A user-friendly exploration interface for interacting with classified volume data.

The remainder of this paper is organized as follows: Section II reviews related work; Section III presents our method; Section IV describes the exploration interface; results and discussion are given in Sections V and VI; and Section VII concludes the paper.

II. Related Works

Various aspects of transfer functions (TFs) have been extensively discussed [1]. We focus on methods that support user interaction in multidimensional TF design, especially those using machine learning, dimensionality reduction, and information visualization.

Multidimensional TFs incorporate multivariate or derived attributes. While multivariate data come directly from acquisition, derived features—such as gradient magnitude, curvature, or texture—are computed from primary data. Selecting relevant attributes is challenging due to the "curse of dimensionality." Dimensionality reduction is a common solution [4]–[8].

Histograms are widely used in 2D TF design [9], often representing intensity–gradient magnitude. Several methods automate histogram-based TFs by grouping spatial regions or combining with clustering algorithms such as affinity propagation [11], hierarchical clustering [12], and self-organizing maps [13].

TF design strategies typically follow two directions: user interfaces for direct manipulation of attributes (e.g., parallel coordinates) [8], [14], or projection-based approaches using MDS or PCA [15]. SOM-based methods [4], [7], [16] perform dimensionality reduction and offer interactive maps of similar voxel regions. Our method shares this philosophy but uses an MDS-based projection and density-based clustering to produce a scatter plot interface.

Supervised learning has also been used in TF design, with approaches based on neural networks [18], [19], GANs [20], [21], and CNNs [2], [22]. Graph-based strategies [23] enhance volume rendering by identifying and emphasizing key structures.

III. Method

This section presents our unsupervised method for TF design, enabling semi-automated material classification and initial TF specification for intuitive volume exploration.

Fig. 1 shows an overview. After organizing the dataset into a volume grid, we apply three steps: dimensionality reduction, clustering, and pivot-based indexing.

A. Dimensionality Reduction

We use FastMap [24] to project high-dimensional data into 2D while preserving clustering structure. The algorithm finds two distant pivots and projects points onto the line between them.

Fig. 1. Overview of the proposed unsupervised method for transfer function definition and design.

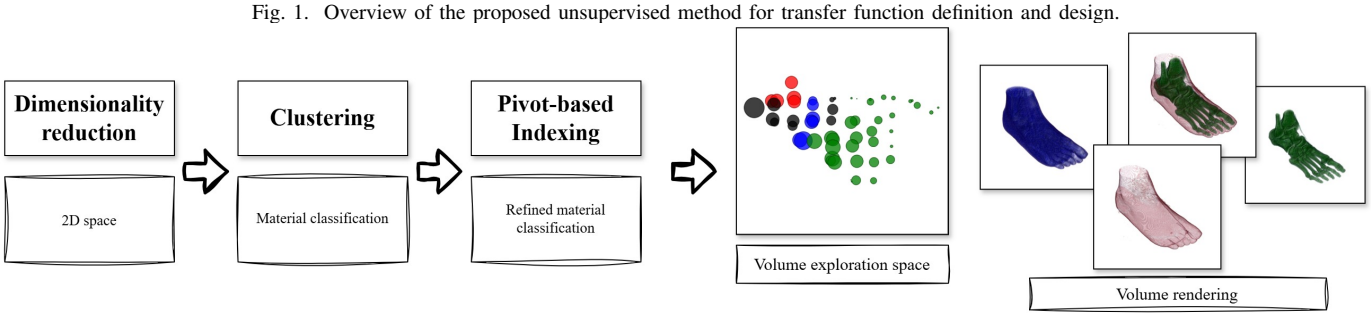

Let d be the number of attributes and n the number of voxels. The steps are:

1) Find two points (pivots) furthest apart.
2) Project points onto a hyperplane orthogonal to the pivots' line.

To avoid quadratic complexity, we use the heuristic from [24] (Algorithm 1) which approximates distant pivots.

Algorithm 1: Pivot searching of FastMap.

Input: $\mathbb{O}$
Output: Pivots O_a, O_b
$O_a \leftarrow$ random point $o \in \mathbb{O}$
$O_b \leftarrow$ point $o \in \mathbb{O}$ farthest from O_a
$O_a \leftarrow$ point $o \in \mathbb{O}$ farthest from O_b

Time complexity is $\mathcal{O}(nk)$ with $k = 2$.

B. Clustering

To simplify classification and highlight details, we use DBSCAN [25]. Since the original has worst-case $\mathcal{O}(n^2)$ complexity, we adopt a grid-based variant [26] with $\mathcal{O}(n \log n)$ complexity.

Parameters $minPts$ and ε must be tuned by the user. The algorithm partitions space into a grid, estimates density, identifies core points, expands clusters, assigns border points, and labels noise.

C. Pivot-based indexing

To reduce scatter plot clutter, we plot only selected pivots within each cluster. Each cluster is subdivided into sub-clusters by assigning points to their nearest pivot (Algorithm 2).

Algorithm 2: Finding sub-clusters within a cluster.

Input: Points $\mathbb{P}$ of cluster c
Input: Pivots $\mathbb{P}_s$ of cluster c
Output: Points with sub-cluster assignment
foreach $p \in \mathbb{P}$ **do**
  $p_s \leftarrow$ nearest pivot in $\mathbb{P}_s$
  Assign p to p_s's sub-cluster
end

We select pivots using Sparse Spatial Selection (SSS) [27], which adds points as pivots if they are sufficiently distant from existing ones, controlled by a distance factor α.

Algorithm 3: Sparse Spatial Selection.

Input: Points $\mathbb{P}$
Output: Selected pivots $\mathbb{P}_s$
$\mathbb{P}_s \leftarrow \{p_1\}$
foreach $p \in \mathbb{P}$ **do**
  if $\forall p_s \in \mathbb{P}_s, dist(p, p_s) \geq M\alpha$ **then**
    $\mathbb{P}_s \leftarrow \mathbb{P}_s \cup \{p\}$
  end
end

Adjusting α controls the number of pivots: smaller α selects more pivots; values near 1 select fewer.

IV. Volume Exploration Space

Figure 2 illustrates the TF design interface, a 2D scatter plot where each circle represents a pivot selected by SSS. The positions from FastMap determine the points' coordinates. Each pivot is a central point of a cluster, with its circle radius proportional to the number of voxels it represents, normalized logarithmically.

Our method generates an initial TF specification using a predefined opacity and a rainbow color scale, assigning a unique color per cluster.

Users adjust the TF following the WYSIWYG principle: pivot color and opacity map directly to their associated voxels according to clustering. Both selected and unselected elements can be customized.

Volume exploration occurs through pivot selection. The system dynamically increases the opacity of selected pivots and decreases that of others. Users can make arbitrary selections, save them as groups, and interact with pivots, clusters, or groups as selectable entities.

Iterative selection of nearby elements aids identifying volume details. FastMap and DBSCAN naturally cluster similar instances spatially, simplifying this process.

Our approach automates material classification by assuming each cluster or pivot represents a relevant item. If unsatisfied, users may select/deselect elements or adjust parameters:

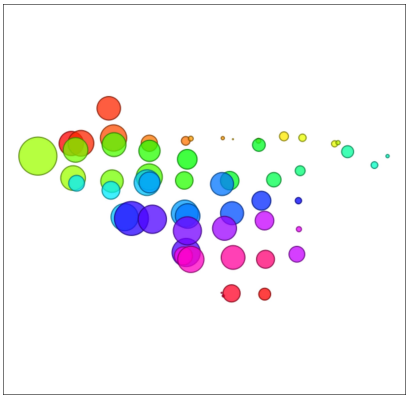

(a) Initial transfer function specification (semi-automatic generated).

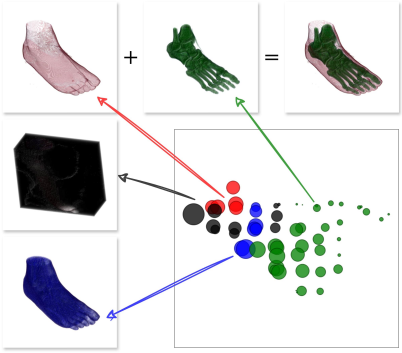

(b) Fine-tune material classification after user adjustment.

Fig. 2. Transfer function design interface and volume exploration space of a right male foot dataset.

- input volume data,
- DBSCAN parameters ε and $minPts$,
- SSS distance factor α.

V. Results

A. Experimental Design

Experiments ran on an Intel Core i5-7200U, 8 GB RAM, Ubuntu 22.04 64-bit, with an NVIDIA GeForce GT 940MX GPU.

We used classical volume ray-casting with Blinn-Phong illumination and trilinear interpolation. Ray step adjusted per voxel spacing. Runtimes are averages of five trials.

The system was implemented in C++ using Qt and CUDA C/C++. The implementation is publicly available.

Table I lists the volume datasets used in experiments.

All volumes contain scalar density values. Multidimensional attributes were derived—13 in total—including intensity, gradient magnitude, Laplacian magnitude, and 10 local histogram statistics (absolute deviation, contrast, energy, entropy, inertia, kurtosis, mean, skewness, standard deviation, variance).

Attribute selection was empirical, tailored per dataset to balance discrimination and computational cost.

B. Runtime

Table II presents runtimes (seconds) for each dataset.

TABLE I
VOLUME DATASETS.

Dataset	Grid size	Total voxels
Engine block	$256 \times 256 \times 256$	16,777,216
Knees	$379 \times 229 \times 305$	26,471,255
Tooth	$256 \times 256 \times 161$	10,551,296

TABLE II
RUNTIME (SECONDS) OF THE PROPOSED METHOD PER DATASET.

	Engine block	Knees	Tooth
Dimensionality reduction	7.50	7.98	36.05
Clustering	51.52	102.77	19.42
Pivot-based indexing	2.23	3.15	1.33
Volume exploration space	1.48	1.86	0.79

C. Data classification

Attribute selection was done empirically by iterative testing and visual assessment, ensuring effective separation of volumetric structures while maintaining computational feasibility.

DBSCAN's $minPts$ was fixed at 4 [25]. Parameter ε varied within $[0.2, 0.35]$, and SSS parameter α within $[0.8, 0.95]$ for volume exploration.

1) Engine block dataset: Figure 3 shows the volume exploration space for the engine block. Each numbered group corresponds to classified volume details in Fig. 4. Parameters: $k = 4$, TF = {intensity, skewness, gradient magnitude, variance}; $minPts = 4$; $\varepsilon = 0.35$; $\alpha = 0.85$.

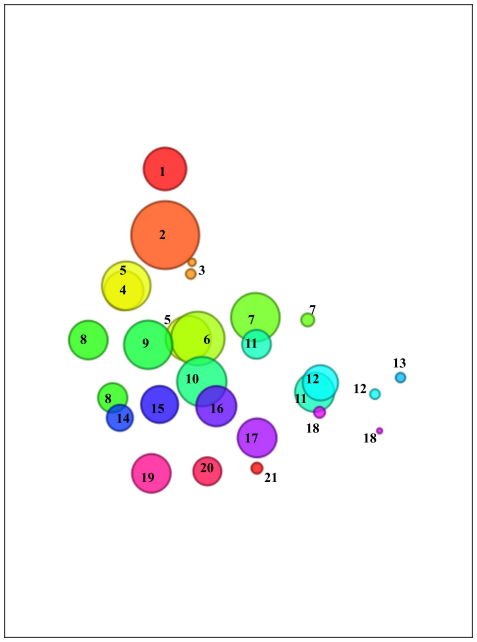

Fig. 3. Volume exploration space for engine block dataset. Parameters: TF = {intensity, skewness, gradient magnitude, variance}; $minPts = 4$; $\varepsilon = 0.35$; $\alpha = 0.85$.

Fig. 4. Rendered classified volume details for engine block. Parameters as in Fig. 3.

Figure 5 shows a volume exploration simulation revealing engine components, starting from Fig. 3.

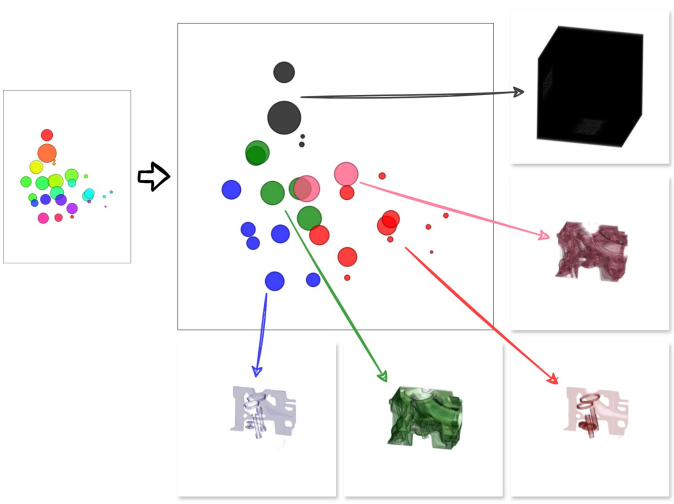

Fig. 5. User-refined transfer function and volume classification for engine block. Groups formed empirically. Parameters as in Fig. 3.

2) Knees dataset: Preliminary classification is shown in Fig. 6 with rendered details in Fig. 7. Parameters: TF = {intensity, variance, absolute deviation, energy, contrast}; $minPts = 4$; $\varepsilon = 0.35$; $\alpha = 0.9$.

Figure 8 illustrates grouped bones and muscles: femur, tibia, patella, fibula, thigh and knee muscles.

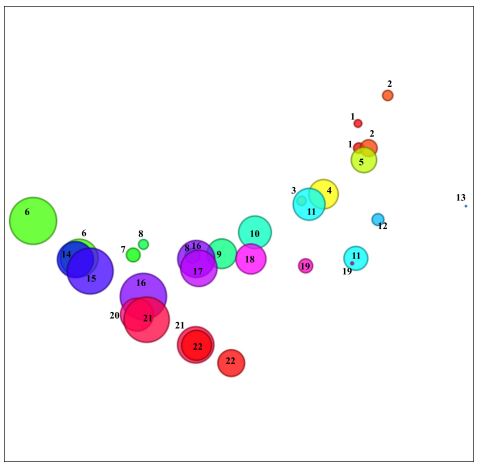

Fig. 6. Volume exploration space for knees dataset. Parameters as above.

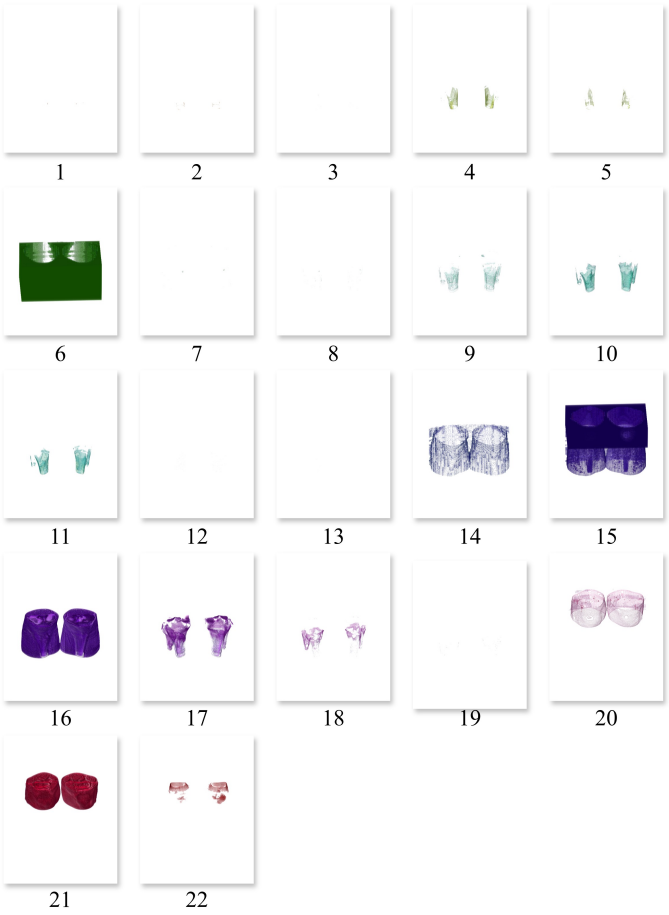

Fig. 7. Rendered classified volume details for knees dataset. Parameters as above.

3) Tooth dataset: Figure 10 shows the volume exploration space, with rendered details in Fig. 10. Parameters: TF = {intensity, variance, absolute deviation, energy, contrast, entropy}; $minPts = 4$; $\varepsilon = 0.23$; $\alpha = 0.9$.

Figure 11 shows empirically grouped tooth structures: enamel, pulp, dentin, crown, entire tooth, and immersion fluid.

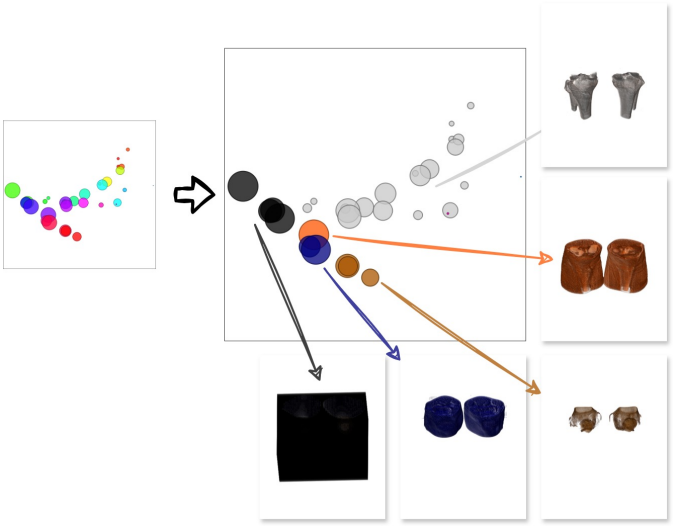

Fig. 8. User-refined TF and classification for knees dataset. Groups formed empirically. Parameters as above.

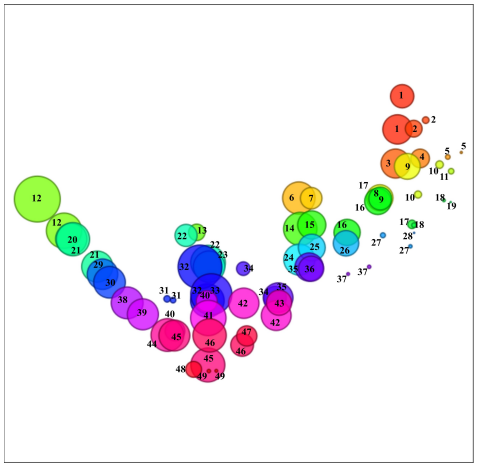

Fig. 9. Volume exploration space for tooth dataset. Parameters as above.

VI. Discussion

The dimensionality reduction approach effectively addresses common challenges in transfer function design by simplifying the data representation. The choice of DBSCAN parameters strongly affects classification outcomes. The $minPts$ parameter can reliably use a default value of 4 [25], given that FastMap reduces the data to a 2D space. However, the ε parameter requires careful tuning: larger values produce fewer but larger clusters, while smaller values result in more numerous, smaller clusters.

The SSS distance factor (α) similarly influences clustering granularity, varying inversely with the number of pivots per cluster.

Overall, the method incurs minimal computational overhead, demonstrating efficient performance and promising scalability for large volumetric datasets.

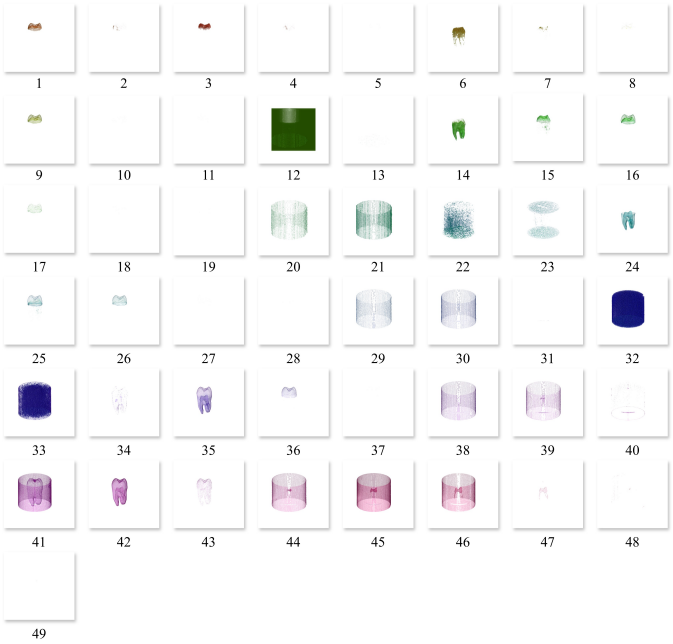

Fig. 10. Rendered classified volume details for tooth dataset. Parameters as above.

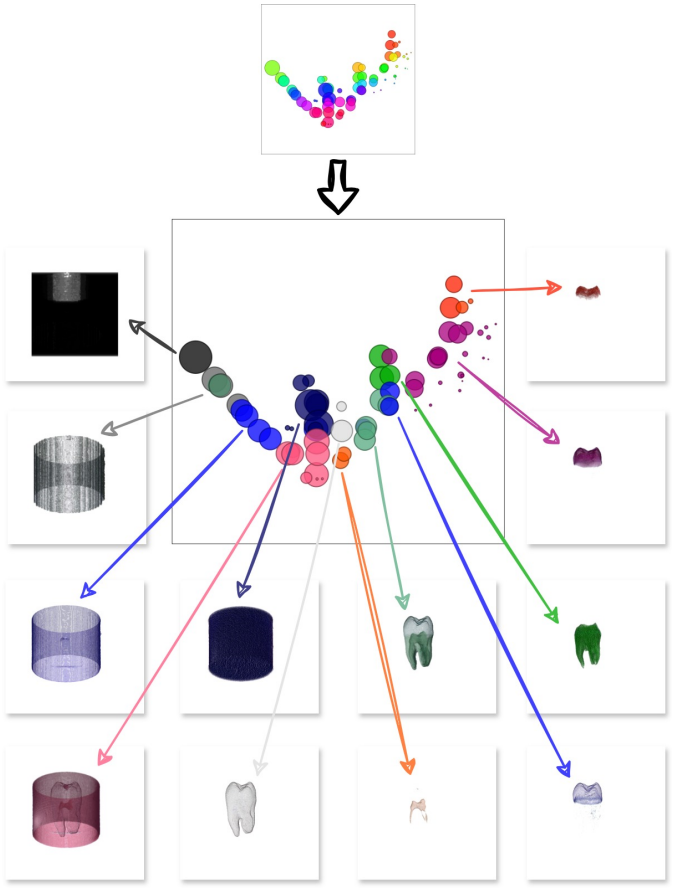

Fig. 11. User-refined TF and classification for tooth dataset. Groups formed empirically. Parameters as above.

VII. Conclusions

We presented a robust method for transfer function (TF) design that integrates feature classification with a simplified volume exploration space. Our approach combines FastMap for efficient feature extraction, DBSCAN for effective clustering, and SSS for pivot-based indexing. These techniques enable semi-automatic classification and initial TF specification, visualized through an intuitive scatter plot interface for volume exploration.

The method exhibits low computational overhead, short runtimes, and minimal storage requirements, highlighting its practicality and scalability for real-world applications. Future work will focus on assessing the method's performance with large, high-dimensional datasets to validate its scalability and effectiveness.

Moreover, we aim to extend our evaluation to multivariate data, enhancing the method's applicability and robustness across a wider range of volume datasets.

Acknowledgements

This work was partially supported by the Brazilian Coordenação de Aperfeiçoamento de Pessoal de Nível Superior (CAPES).

References

[1] P. Ljung, J. Krüger, E. Groller, M. Hadwiger, C. D. Hansen, and A. Ynnerman, "State of the art in transfer functions for direct volume rendering," in *Computer graphics forum*, vol. 35, no. 3. Wiley Online Library, 2016, pp. 669–691.

[2] B. Pan, J. Lu, H. Li, W. Chen, Y. Wang, M. Zhu, C. Yu, and W. Chen, "Differentiable design galleries: A differentiable approach to explore the design space of transfer functions," *IEEE Transactions on Visualization and Computer Graphics*, vol. 30, no. 1, pp. 1369–1379, 2024.

[3] S. Arens and G. Domik, "A survey of transfer functions suitable for volume rendering." in *VG@ Eurographics*, 2010, pp. 77–83.

[4] L. Cai, B. P. Nguyen, C.-K. Chui, and S.-H. Ong, "A two-level clustering approach for multidimensional transfer function specification in volume visualization," *Vis. Comput.*, vol. 33, no. 2, p. 163–177, feb 2017. [Online]. Available: https://doi.org/10.1007/s00371-015-1167-y

[5] A. Abbasloo, V. Wiens, M. Hermann, and T. Schultz, "Visualizing tensor normal distributions at multiple levels of detail," *IEEE Transactions on Visualization and Computer Graphics*, vol. 22, no. 1, pp. 975–984, 2016.

[6] Y. Gao, C. Chang, X. Yu, P. Pang, N. Xiong, and C. Huang, "A vr-based volumetric medical image segmentation and visualization system with natural human interaction," *Virtual Real.*, vol. 26, no. 2, p. 415–424, jun 2022. [Online]. Available: https://doi.org/10.1007/s10055-021-00577-4

[7] F. D. M. Pinto and C. M. D. S. Freitas, "Design of multi-dimensional transfer functions using dimensional reduction," in *Proceedings of the 9th Joint Eurographics/IEEE VGTC conference on Visualization*, 2007, pp. 131–138.

[8] X. Zhao and A. Kaufman, "Multi-dimensional reduction and transfer function design using parallel coordinates," in *Volume graphics. International Symposium on Volume Graphics*. NIH Public Access, 2010, p. 69.

[9] J. Kniss, G. Kindlmann, and C. Hansen, "Multidimensional transfer functions for interactive volume rendering," *IEEE Transactions on visualization and computer graphics*, vol. 8, no. 3, pp. 270–285, 2002.

[10] S. Roettger, M. Bauer, and M. Stamminger, "Spatialized transfer functions," in *Proceedings of the Seventh Joint Eurographics / IEEE VGTC Conference on Visualization*, ser. EUROVIS'05. Goslar, DEU: Eurographics Association, 2005, p. 271–278.

[11] T. Zhang, Z. Yi, J. Zheng, D. C. Liu, W.-M. Pang, Q. Wang, J. Qin *et al.*, "A clustering-based automatic transfer function design for volume visualization," *Mathematical Problems in Engineering*, vol. 2016, 2016.

[12] P. Sereda, A. Vilanova, and F. A. Gerritsen, "Automating transfer function design for volume rendering using hierarchical clustering of material boundaries." in *EuroVis*, 2006, pp. 243–250.

[13] F.-Y. Tzeng and K.-L. Ma, "A cluster-space visual interface for arbitrary dimensional classification of volume data," in *Proceedings of the Sixth Joint Eurographics - IEEE TCVG Conference on Visualization*, ser. VISSYM'04. Goslar, DEU: Eurographics Association, 2004, p. 17–24.

[14] M. Tory, S. Potts, and T. Moller, "A parallel coordinates style interface for exploratory volume visualization," *IEEE Transactions on Visualization and Computer Graphics*, vol. 11, no. 1, pp. 71–80, 2005.

[15] H. Guo, H. Xiao, and X. Yuan, "Multi-dimensional transfer function design based on flexible dimension projection embedded in parallel coordinates," in *2011 IEEE Pacific Visualization Symposium*. IEEE, 2011, pp. 19–26.

[16] N. M. Khan, M. Kyan, and L. Guan, "Intuitive volume exploration through spherical self-organizing map and color harmonization," *Neurocomputing*, vol. 147, pp. 160–173, 2015.

[17] L. Wang, X. Zhao, and A. E. Kaufman, "Modified dendrogram of attribute space for multidimensional transfer function design," *IEEE transactions on visualization and computer graphics*, vol. 18, no. 1, pp. 121–131, 2011.

[18] F.-Y. Tzeng, E. B. Lum, and K.-L. Ma, "An intelligent system approach to higher-dimensional classification of volume data," *IEEE Transactions on visualization and computer graphics*, vol. 11, no. 3, pp. 273–284, 2005.

[19] L. Wang, X. Chen, S. Li, and X. Cai, "General adaptive transfer functions design for volume rendering by using neural networks," in *International Conference on Neural Information Processing*. Springer, 2006, pp. 661–670.

[20] M. Berger, J. Li, and J. A. Levine, "A generative model for volume rendering," *IEEE transactions on visualization and computer graphics*, vol. 25, no. 4, pp. 1636–1650, 2018.

[21] F. Hong, C. Liu, and X. Yuan, "Dnn-volvis: Interactive volume visualization supported by deep neural network," in *2019 IEEE Pacific Visualization Symposium (PacificVis)*. IEEE, 2019, pp. 282–291.

[22] S. Kim, Y. Jang, and S.-E. Kim, "Image-based tf colorization with cnn for direct volume rendering," *IEEE Access*, vol. 9, pp. 124 281–124 294, 2021.

[23] O. Sharma, T. Arora, and A. Khattar, "Graph-based transfer function for volume rendering," in *Computer Graphics Forum*, vol. 39, no. 1. Wiley Online Library, 2020, pp. 76–88.

[24] C. Faloutsos and K.-I. Lin, "Fastmap: A fast algorithm for indexing, data-mining and visualization of traditional and multimedia datasets," in *Proceedings of the 1995 ACM SIGMOD international conference on Management of data*, 1995, pp. 163–174.

[25] M. Ester, H.-P. Kriegel, J. Sander, X. Xu *et al.*, "A density-based algorithm for discovering clusters in large spatial databases with noise," in *kdd*, vol. 96, no. 34, 1996, pp. 226–231.

[26] A. Gunawan and M. de Berg, "A faster algorithm for dbscan," *Master's thesis*, 2013.

[27] O. Pedreira and N. R. Brisaboa, "Spatial selection of sparse pivots for similarity search in metric spaces," in *International Conference on Current Trends in Theory and Practice of Computer Science*. Springer, 2007, pp. 434–445.